BBA - Bioenergetics 1858 (2017) 966–974

Contents lists available at ScienceDirect

BBA - Bioenergetics

journal homepage: www.elsevier.com/locate/bbabio

A γ-subunit point mutation in *Chlamydomonas reinhardtii* chloroplast F_1F_o-ATP synthase confers tolerance to reactive oxygen species

Felix Buchert[a,b,*], Benjamin Bailleul[b], Toru Hisabori[a]

[a] Laboratory for Chemistry and Life Science, Tokyo Institute of Technology, Nagatsuta 4259-R1-8, Midori-ku, Yokohama 226-8503, Japan
[b] Institut de Biologie Physico-Chimique, UMR 7141 CNRS-UPMC, 13 rue Pierre et Marie Curie, 75005 Paris, France

ARTICLE INFO

Keywords:
Chloroplast F_1F_o-ATP synthase
Photosynthesis
Reactive oxygen species

ABSTRACT

The chloroplast F_1F_o-ATP synthase (CF_1F_o) drives ATP synthesis and the reverse reaction of ATP hydrolysis. The enzyme evolved in a cellular environment where electron transfer processes and molecular oxygen are abundant, and thiol modulation in the γ-subunit *via* thioredoxin is important for its ATPase activity regulation. Especially under high light, oxygen can be reduced and forms reactive oxygen species (ROS) which can oxidize CF_1F_o among various other biomolecules. Mutation of the conserved ROS targets resulted in a tolerant enzyme, suggesting that ROS might play a regulatory role. The mutations had several side effects *in vitro*, including disturbance of the ATPase redox regulation [F. Buchert et al., Biochim. Biophys. Acta, 1817 (2012) 2038–2048]. This would prevent disentanglement of thiol- and ROS-specific modes of regulation. Here, we used the F_1 catalytic core *in vitro* to identify a point mutant with a functional ATPase redox regulation and increased H_2O_2 tolerance. In the next step, the mutation was introduced into *Chlamydomonas reinhardtii* CF_1F_o, thereby allowing us to study the physiological role of ROS regulation of the enzyme *in vivo*. We demonstrated in high light experiments that CF_1F_o ROS targets were involved in the significant inhibition of ATP synthesis rates. Molecular events upon modification of CF_1F_o by ROS will be considered.

1. Introduction

In the course of evolution, the F-ATP synthase (F_1F_o) has been remarkably conserved in terms of structure and function [reviewed in 1]. The enzyme is embedded in energy-producing membranes of bacteria, mitochondria and chloroplasts. The chloroplasts F_1F_o (CF_1F_o) consists of two portions, the membrane-attached F_1 with five subunits ($\alpha_3\beta_3\gamma\delta\varepsilon$), and the membrane-spanning F_o with four subunits (abb'c_{14}). At the expense of a *trans*-thylakoid electrochemical proton gradient ($\Delta\tilde{\mu}_{H^+}$), ATP is produced from inorganic phosphate and ADP at the catalytic sites, mainly located in β-subunits. Several mechanisms regulate the activity of CF_1F_o and are believed to be important for the optimization of photosynthetic activity. The first one is a regulation by the substrate itself, the $\Delta\tilde{\mu}_{H^+}$. A $\Delta\tilde{\mu}_{H^+}$ threshold level, $\Delta\tilde{\mu}_{H^+trigger}$, is necessary to transition CF_1F_o into an active state in isolated chloroplasts [2,3]. This transition has also been demonstrated *in vivo* [4,5] by using electrochromic shift (ECS) measurements [reviewed in 6]. Dissipation of $\Delta\tilde{\mu}_{H^+}$ *via* CF_1F_o is achieved by protonation and deprotonation of a Glu residue in the c-subunit, eventually driving rotation of subunits $\gamma\varepsilon c_{14}$ against the static subunits, $\alpha_3\beta_3\delta$abb'. The static β- and the rotating γ-subunit share temporary contacts during the catalytic cycle, probably guided by ionic interactions [7,8]. F_1F_o also catalyzes the reverse reaction by generating a $\Delta\tilde{\mu}_{H^+}$ upon ATP hydrolysis. Both isolated F_1 and the catalytic core $\alpha_3\beta_3\gamma$ perform ATP hydrolysis *in vitro*. Other mechanisms are involved in ATPase activity regulation and have been investigated especially *in vitro*. Tightly bound MgADP on the catalytic sites produces low ATPase rates, which is referred to as ADP inhibition [9]. Anions [10] and detergents like LDAO [11] can alleviate ADP inhibition by facilitating the release of MgADP from the catalytic sites. Besides the ε-subunit with its intrinsic ATPase inhibitor function [12], CF_1F_o has a unique feature located in the γ-subunit. A short segment harbors a disulfide that can be reduced by thioredoxin, thereby unmasking ATPase activity [13]. This mechanism is referred to as ATPase redox regulation. Insertion of the corresponding spinach γ-fragment

Abbreviations: F_1F_o, F_1F_o-ATP synthase; CF_1F_o, chloroplast F_1F_o-ATP synthase; $F_{1\text{-redox}}$, redox-sensitive F_1 derived from the $\alpha_3\beta_3\gamma$ complex of *T. elongatus* BP-1; γMLCA, set of mutations in the $F_{1\text{-redox}}$ γ-subunit γM24L/γC90A/γM280L/γM283L; ROS, reactive oxygen species; Trx, thioredoxin; LDAO, *N*-dimethyldodecylamine-N-oxide; PSI, photosystem I; PSII, photosystem II; P_i, inorganic phosphate; DCMU, 3-(3,4-dichlorophenyl)-1,1-dimethylurea; HA, hydroxylamine; ECS, electrochromic shift; $\Delta\tilde{\mu}_{H^+}$, *trans*-thylakoid electrochemical proton gradient; ΔΨ, electric field component of the $\Delta\tilde{\mu}_{H^+}$; $\Delta\tilde{\mu}_{H^+dark}$, $\Delta\tilde{\mu}_{H^+}$ established in dark-adapted samples *via* ATP hydrolysis by CF_1F_o; $\Delta\Delta\tilde{\mu}_{H^+}$ and ΔΔΨ, light-induced changes of $\Delta\tilde{\mu}_{H^+}$ and ΔΨ, respectively, compared to values in the dark; $\Delta\tilde{\mu}_{H^+trigger}$, a critical threshold $\Delta\tilde{\mu}_{H^+}$ to be exceeded for triggering high CF_1F_o activity

* Corresponding author at: Institut de Biologie Physico-Chimique, UMR 7141 CNRS-UPMC, 13 rue Pierre et Marie Curie, 75005 Paris, France.
E-mail address: buchert@ibpc.fr (F. Buchert).

http://dx.doi.org/10.1016/j.bbabio.2017.09.001
Received 6 June 2017; Received in revised form 11 August 2017; Accepted 5 September 2017
Available online 07 September 2017
0005-2728/

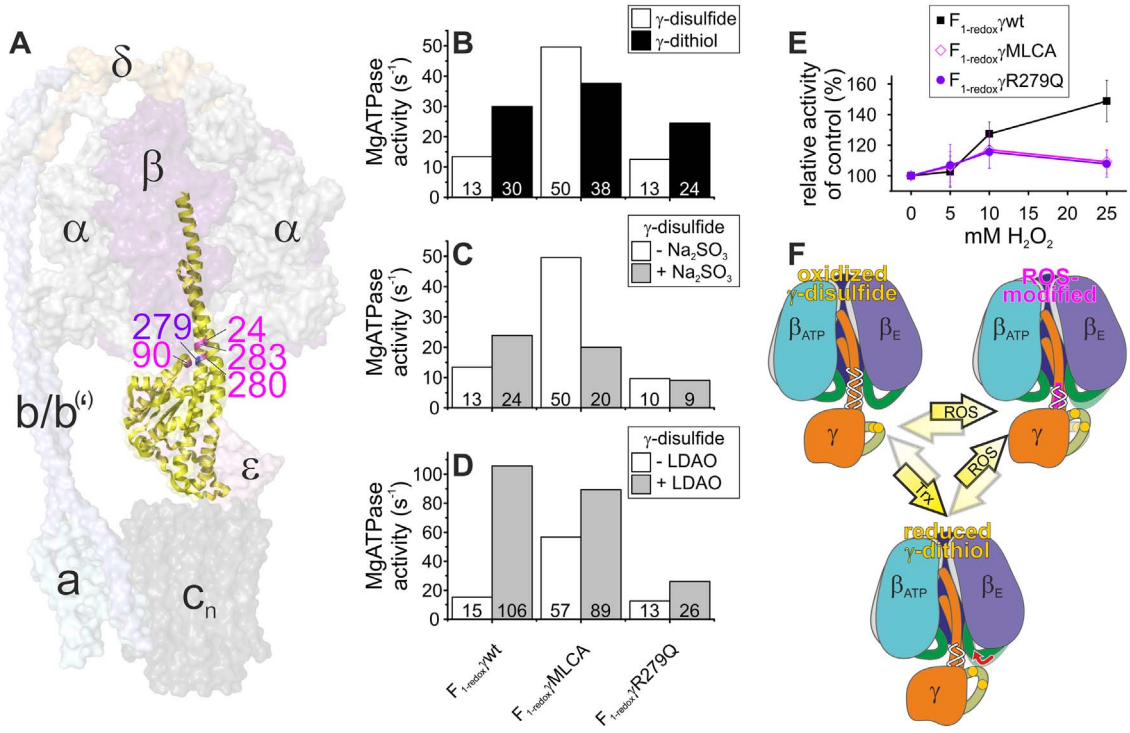

Fig. 1. Highlighting the position of mutations, regulatory features in mutant $F_{1\text{-redox}}$ MgATPase activity assays, and the mechanistic model upon γ-subunit modifications. (A) The positions of mutated γ-residues with $F_{1\text{-redox}}$ numbering are shown in *E. coli* F_1F_o cryo-EM structure [37, PDB 5T4P]. The γ-subunit is presented as cartoon, with sulfur-containing residues in magenta and the Arg in violet. Other subunits are semitransparent surface representations. The b'-subunit is found in chloroplasts and stoichiometry of the subunit c-ring is dependent on the species. (B) $F_{1\text{-redox}}$ MgATPase regulation upon chemical modification of the γ-subunit redox state. ATP hydrolysis rates in the presence of substrate-coordinating Mg^{2+} are expressed MgATPase activity in s^{-1}. (C) Overcoming ADP inhibition by addition of 20 mM Na_2SO_3. (D) Cancelling ADP inhibition by addition of 0.1% *v/v* LDAO. (E) Impact of H_2O_2 on MgATPase activity under γ-disulfide-promoting conditions ($n = 3$, ± SD). (F) The model of ATPase redox regulation and functional modification by ROS in $F_{1\text{-redox}}$ shows the altered interactions of the γ-subunit (orange) with the β-subunit (β_E and β_{ATP} are the empty and ATP-bound states, respectively). Reduction of regulatory Cys couple (yellow balls) by thioredoxin (Trx) induces steric repulsion between the extended γ-redox domain (olive) and the βDELSEED-loop (green). Then, reorientation of the DELSEED-loop (red arrow) modulates the interface with the γ-subunit neck region. Thereby, relative slippage of the helical γ-termini (twisted white lines) is restricted [15]. Such a restriction results in elevated MgATPase activity due to lowered ADP inhibition efficiency in the F_1 enzyme without inserted γ-redox domain [24]. Upon oxidation of sulfurous γ-targets by ROS (magenta), restricted relative slippage of the γ-termini lowered the ADP inhibition propensity in $F_{1\text{-redox}}$, thus stimulating MgATPase activity. Independently of the γ-dithiol, ROS-mediated modulation of γ-terminal movements might inhibit MgATPase activity in the chloroplast enzyme [17].

transferred the CF_1F_o-specific redox regulation feature to a cyanobacterial F_1 enzyme [14]. The engineered F_1, termed $F_{1\text{-redox}}$ in this study, helped to identify a redox regulation interface between the β- and γ-subunit distant from the γ-dithiol [15]. This subunit interface plays an important role in torque generation [16]. It also makes CF_1F_o susceptible to activity impairment upon exposure to reactive oxygen species (ROS) since it harbors a conserved set of sulfur-containing Met and Cys residues [17]. The *in vitro* target study used a hybrid F_1 system with spinach CF_1 γ-subunit and *R. rubrum* F_1 $\alpha_3\beta_3$ heterohexamer. Removal of the redox-regulatory Cys pair did not change ROS effects, indicating that the γ-disulfide formation is not involved in ROS-mediated ATPase activity loss. However, the ROS-resistant mutants had lost ATPase redox regulation.

The main focus of this report is the ROS-mediated regulation of ATP synthesis rates under high light *in vivo*. ROS production during photosynthesis is inevitable as molecular oxygen can accept electrons *via* a multitude of processes [reviewed in 18]. Therefore, various ROS detoxification mechanisms exist such as the Mehler reaction where, under high light, superoxide anion radicals are produced that are subsequently detoxified in the water-water cycle yielding H_2O_2 as an intermediate to be further detoxified [19,20]. ROS-mediated protein modifications usually involve oxidation of Met, Cys, and aromatic residues which, to a certain extent, can be reversible [reviewed in 21]. Studying the specific regulation of CF_1F_o activity by ROS *in vivo* requires the design of a resistant mutant that displays no side effects regarding the other modes of regulation, *e.g.*, *via* γ-disulfide formation/cleavage. The functional redox-regulatory feature is necessary since the extent of activity impairment by singlet oxygen exposure depended on the γ-subunit redox state in spinach thylakoids [22].

In this study, a point mutation of a conserved γ-subunit Arg yielded an alternative ROS-resistant F_1 enzyme *in vitro* that displayed normal ATPase redox regulation. Thus, by eliminating the major drawback of previous *in vitro* mutants, this allowed transition to *in vivo* measurements. By using *Chlamydomonas reinhardtii*, we conferred H_2O_2 tolerance to an *in vivo* system and analyzed the consequences of this ROS tolerance upon high light treatment of the cells. We observed a high light-induced slowdown of the wild type enzyme which could play an important role in the $\Delta\tilde{\mu}_{H^+}$-dependent regulation of photosynthesis that would be prevented in the mutant. This significant inhibition occurred independently of the $\Delta\tilde{\mu}_{H^+}$ regulation. On this basis, we propose a molecular scenario for ROS-modified CF_1F_o and a preliminary outline on bioenergetic consequences.

2. Materials and methods

2.1. Materials

Aldrithiol-2, ATP, pyruvate kinase, lactate dehydrogenase, and phosphoenolpyruvate were purchased from Sigma. NADH was purchased from Roche Diagnostics. Other chemicals were of the highest grade commercially available. Inhibitors were added from 1000 × stock solutions.

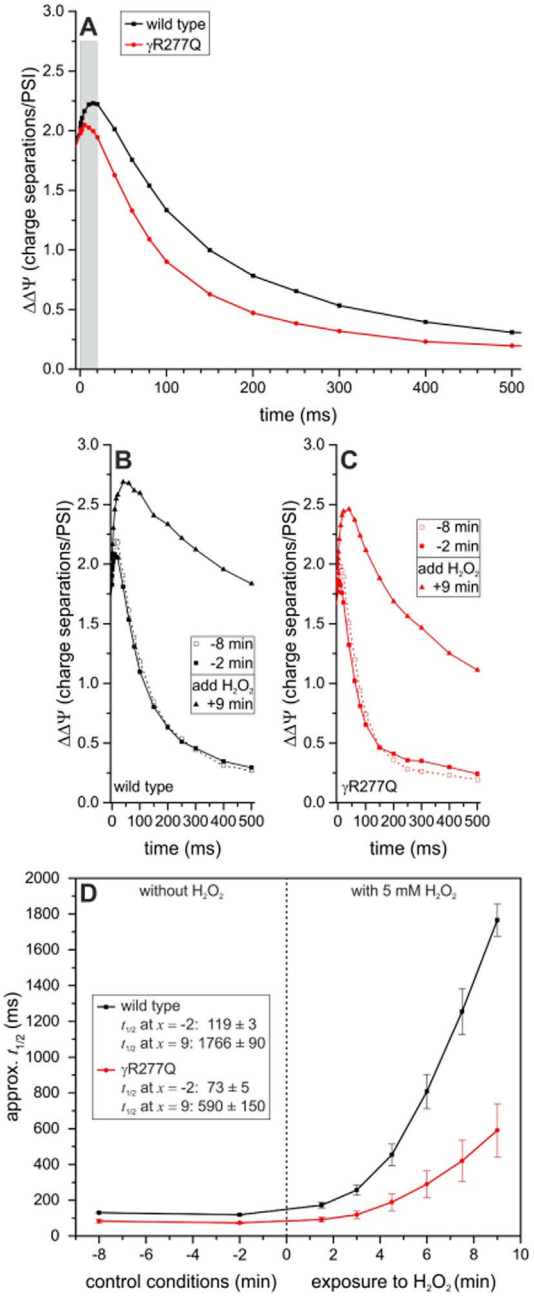

Fig. 2. *C. reinhardtii* CF_1F_o activity in the dark probed by flash-induced ECS signal decay and the impact of exogenously added H_2O_2. (A) Representative 500-ms ECS decay phases illustrate CF_1F_o activity. The "b" phase in the 20 ms-range is highlighted in gray and explained in Section 3.2. Refer also to Fig. S2 for demonstration of the "b" phase upon on CF_1F_o inhibition. Incubation with 5 mM H_2O_2 slowed down the ECS decay in both (B) wild type and (C) γR277Q. (D) The H_2O_2 treatment slowed down the initial ECS decay about twice as much in the wild type (14.8-fold) as compared to the mutant (8.1-fold). Numbers were calculated from the half-time of ECS decay, starting from signals at the end of the "b" phase (expressed in ms; $n = 3$, ± SD).

2.2. In vitro studies: Bacterial expression vectors, recombinant protein purification, ATPase activity measurements, and post-translational enzyme modifications

Escherichia coli strains DH5α were used for cloning and BL21(DE3) uncΔ702 [23] were used for expression of the $\alpha_3\beta_3\gamma$ complex of *T. elongatus* BP-1, respectively. The latter strain was a kind gift from Dr. C. S. Harwood (University of Iowa). For *in vitro* studies, a *T. elongatus* BP-1 $F_{1\text{-redox}}$ chimera enzyme was used that showed plant-specific redox modulation of ATP hydrolysis upon insertion of a Cys-containing fragment from spinach CF_1 into a cyanobacterial γ-subunit [14]. The used plasmid constructs, the mutant $F_{1\text{-redox}}$γMLCA (γM24L/γC90A/γM280L/γM283L), and the purification protocol were published previously [15]. In order to generate $F_{1\text{-redox}}$γR279Q, abutting forward (5'ATGACGGCAATGAACAACGCCAG) and reverse primers (5'CTGTGCCGCCAATTCTGAGG) were used. As described previously [15], cleavage (50 mM DTT) and formation (0.5 mM Aldrithiol-2) of the γ-subunit disulfide was promoted prior to ATP hydrolysis measurements in a regenerating assay [24]. ATP hydrolysis rates in the presence of substrate-coordinating Mg^{2+} [25] are referred to as MgATPase activity. In some experiments the addition of LDAO [11,26] and sodium sulfite [10], respectively, served to favor the release of tightly bound MgADP, thus enhancing ATP hydrolysis rates. Where indicated, H_2O_2 pretreatment was carried out as described previously [17].

2.3. Nuclear transformation and growth of Chlamydomonas reinhardtii cultures

EST clones were ordered from www.kazusa.or.jp (Accession No. AV634065). The *ATPC* CDS was cloned as a *Bam*HI/*Eco*RI fragment into the pPEARL expression vector (GenBank: KU531882.1) by using forward (5'GCCAGGATCCTTAGCCCGAGGTGGCGGCG) and reverse primers (5'GTTCGAATTCATGGCCGCTATGCTCGCC). The latter oligonucleotide was used in combination with a mutational primer (5'CGAGCTGGCTGCCCAGATGAACGCCATG) to generate a megaprimer [27] that harbored γR277Q (*C. reinhardtii* numbering). A non-phototrophic mutant that did not accumulate *ATPC* transcripts [28] served as a recipient strain cultured on TAP medium [29]. Transformants were obtained by electroporation [30] using 25 μF and 1000 V cm^{-1}. Expression of wild type and γR277Q *ATPC* transgene restored phototrophic growth. For this study, transformants were cultured at 50 μmol photons $m^{-2}\,s^{-1}$ on agar-supplemented and liquid minimum medium [29]. Before physiological experiments, liquid cultures were bubbled with sterile air at 50 μmol photons $m^{-2}\,s^{-1}$ constant light, and kept in the exponential phase (0.5–3 × 10^6 cells/mL) at 23 °C by dilutions every 1–2 days. Where indicated, early log-phase cultures were illuminated for 90 min at 800 μmol photons $m^{-2}\,s^{-1}$ under agitation and air bubbling.

2.4. Spectroscopy

C. reinhardtii cultures were harvested and concentrated by centrifugation (3 min, 7500 rpm), and adjusted to 1 × 10^7 cells/mL in minimum medium supplemented with 10% (*w/v*) Ficoll to minimize baseline drifts by phototaxis and sedimentation. The samples were shaken vigorously in the dark for at least 15 min before transferring to the cuvette. *In vivo* photosynthetic parameters were measured at room temperature in a JTS-10 spectrophotometer (Biologic, France) using a similar setup as described previously [31]. Dark-adapted samples were illuminated by a single-turnover laser flash or a short saturating light pulse. The illumination generated an electric field (ΔΨ) due to promotion of charge separation at the level of photosystem I (PSI) and photosystem II (PSII), as well as H^+ translocation coupled to the electron transfer within the cytochrome b_6f complex [4,32]. Changes of the electrochromic shift (ECS) were measured at 520 nm–546 nm, thus eliminating the contribution of cytochromes and scattering effects. The light-induced *trans*-membrane difference potential, hereinafter referred to as membrane potential, was estimated from the ECS amplitudes which are linearly proportional to the ΔΨ component of the $\Delta\tilde{\mu}_{H^+}$ [32]. As described previously [4], flash-induced ECS comprises various phases: a fast increase phase associated with photochemistry in PSI and PSII, which is completed in < 100 μs ("a" phase), and a slow increase phase in the ms range, which corresponds to the turnover of the cytochrome b_6f ("b" phase). After the "b" phase, the ECS signals decay mainly due to ATP synthesis by H^+ translocation *via* CF_1F_o. In dark-adapted samples illuminated by a single-turnover flash, the ECS signal

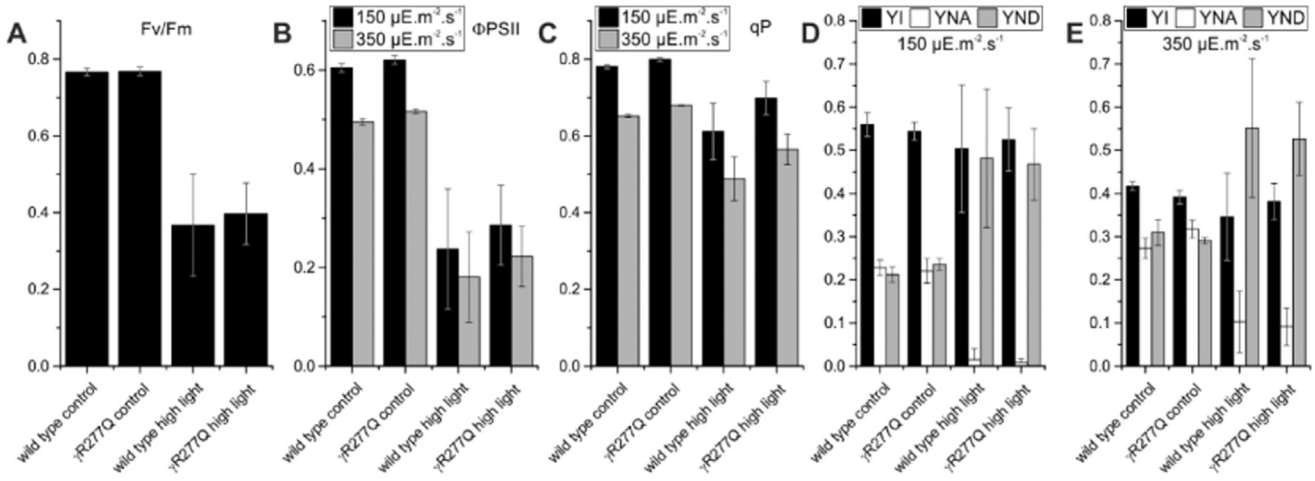

Fig. 3. Determination of photosynthetic parameters in control and high light-treated *C. reinhardtii* CF_1F_o wild type and γR277Q. Results are shown as means of three transformants ± SD and representative kinetics are shown in Fig. S1. (A) The maximum quantum efficiency of PSII, Fv/Fm, is shown and was averaged at two actinic light intensities which were used to calculate (B) the photochemical quantum yield of PSII, ΦPSII, and (C) the PSII efficiency factor, qP. Redox kinetics of P700 were calculated during 5 s illumination with (D) 150 and (E) 350 $\mu E \cdot m^{-2} \cdot s^{-1}$ actinic red light, respectively. The quantum yield of PSI (YI), electron donor side limitation (YND) and acceptor side limitation (YNA) are indicated.

Table 1
Spectroscopic determination of photodamage upon high light treatment.

	(PSI + PSII)/PSI		HL-induced loss of				(PSI + PSII)/PSI		HL-induced loss of		
			PSII[a]	PSI					PSII[a]	PSI	
Wild type	LL	HL		ECS[b]	$P700^{+}$[c]	γR277Q	LL	HL		ECS[b]	$P700^{+}$[c]
#1	1.99	1.22	84%	28%	24%	#1	2.01	1.46	67%	27%	24%
#2	2.06	1.32	80%	31%	34%	#2	2.03	1.29	80%	30%	30%
#3	1.93	1.44	66%	28%	26%	#3	2.04	1.43	73%	35%	34%
mean	2.00	1.33	76%	29%	28%	mean	2.02	1.40	73%	31%	29%
SD	0.06	0.11	10%	2%	5%	SD	0.01	0.09	7%	4%	5%

Inhibitors were 10 µM DCMU + 1 mM HA.

[a] Calculated from the PSII contribution to the flash-induced "a" phase ECS amplitude (*ΔECS*) in high light (HL) and control samples, $1-(\Delta ECS_{\text{HL-inhibitors}} - \Delta ECS_{\text{HL + inhibitors}})/(\Delta ECS_{\text{control-inhibitors}} - \Delta ECS_{\text{control + inhibitors}})$.

[b] Calculated from the PSI contribution of *ΔECS* in HL and control samples, $1-(\Delta ECS_{\text{HL + inhibitors}}/\Delta ECS_{\text{control + inhibitors}})$.

[c] Maximal $P700^{+}$ oxidation calculated from the *ΔI/I* amplitude at 705 nm–730 nm upon a saturating actinic light pulse in presence of PSII inhibitors (ΔP^{+}), $1-(\Delta P^{+}_{\text{HL}}/\Delta P^{+}_{\text{control}})$.

after completion of the "b" phase was used for calculation of CF_1F_o ATP synthesis activity *via* the reciprocal of the ECS decay half-time. The "a" phase in the presence of the PSII inhibitors DCMU (10 µM) and HA (1 mM) was measured at the end of each experiment and used to calibrate ECS signals to one charge separation per PSI. In fluorescence assays the maximum quantum yield (Fv/Fm), the photochemical quantum yield (ΦPSII = (Fm − Fstat)/Fm), and the efficiency factor (qP = (ΦPSII*Fm)/Fv) were measured at two light intensities (red actinic light peaking at 629 nm) [33]. Fv was calculated from Fm − F0, whereas F0, Fstat, and Fm are the fluorescence in darkness, during steady-state illumination, and at the end of a saturating light pulse, respectively. Redox changes of P700 upon actinic illumination were carried out as described previously [34,35] and differentially measured at 705 nm–730 nm to eliminate signals from plastocyanin and scattering effects. Representative fluorescence and P700 absorbance kinetics are shown in Fig. S1.

3. Results and discussion

3.1. The $F_{1\text{-}redox}$ system is an in vitro tool to identify alternative ROS-resistant mutants

The heterologously expressed $F_{1\text{-redox}}$ enzyme was designed to study ATPase redox regulation, exclusively found in the chloroplast enzyme [14]. In $F_{1\text{-redox}}$, a cyanobacterial F_1 $\alpha_3\beta_3\gamma$ complex, the regulatory Cys-containing fragment from spinach CF_1 γ-subunit was inserted. Here, the enzyme was used as a tool in a follow-up study that links ROS tolerance of F_1 ATPase activity to a set of mutations [17], referred to as γMLCA (γM24L/γC90A/γM280L/γM283L). The mutations showed additional effects by perturbing ATPase redox regulation, although the γ-disulfide formation and cleavage was not hampered [15]. Numerous second-site mutations in $F_{1\text{-redox}}$γMLCA background failed to re-establish the regulatory feature, most likely because the primary ROS targets are found in a delicate β/γ-subunit interface that is involved in ATPase redox regulation. In addition to the redox-regulatory disturbance, the γM24 substitution in the γMLCA mutant bears a potential risk to perturb the coupling of H^{+} translocation from nucleotide catalysis *in vivo*, as shown for *E. coli* F_1F_o [36]. Therefore, an alternative approach was carried out without mutating primary ROS targets. We found the $F_{1\text{-redox}}$γR279Q mutant (Fig. 1A) showing wild type-like ATPase redox regulation (Fig. 1B) while displaying different responses to sulfite (Fig. 1C) and LDAO (Fig. 1D). The redox-insensitive $F_{1\text{-redox}}$γMLCA with modified ADP inhibition served as a reference [15]. The chemicals are known to alleviate ADP inhibition, as shown by the 1.8- and 7.1-fold ATPase activity stimulation in the wild type for sulfite and LDAO, respectively. Both approaches failed to enhance $F_{1\text{-redox}}$γR279Q ATPase activity in a wild type-like manner. While sulfite was slightly inhibiting, LDAO enhanced the ATPase activity by a factor 2, a trend that was also observed in $F_{1\text{-redox}}$γMLCA. The $F_{1\text{-redox}}$γMLCA in our follow-up ROS response study can be compared with the previously reported homologous mutant consisting of recombinant spinach CF_1 γ-subunit and *R. rubrum* F_1 $\alpha_3\beta_3$ heterohexamer [17]. Before focusing on the ROS effect of $F_{1\text{-redox}}$,

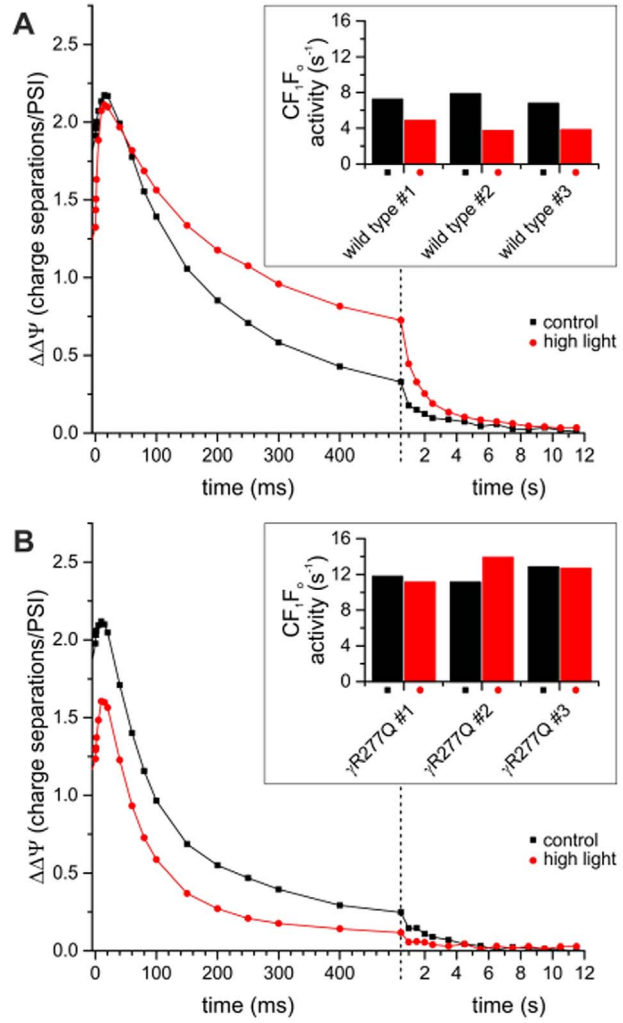

Fig. 4. Partial inhibition of wild type CF_1F_o activity after high light treatment, probed by ECS decay of *C. reinhardtii* cells. (A) Wild type and (B) γR277Q transformants were assayed and representative kinetics are shown with CF_1F_o activity derived from the reciprocal half-time decay of ECS signals after finishing the "b" phase (expressed in s^{-1}; see insets). For more details see Section 3.3.

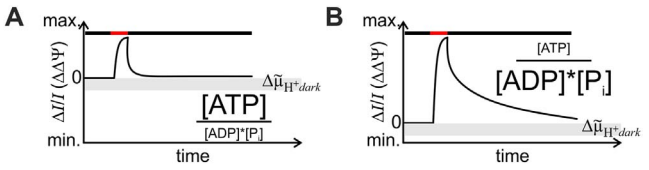

Fig. 5. The basic principle of saturating pulse-induced ECS decay measurements. The data analysis relies on the assumption that, in first approximation, ΔΨ changes upon short saturating light pulses (ΔΔΨ) can be regarded as light-induced $\Delta\tilde{\mu}_{H^+}$ changes. Although $\Delta\tilde{\mu}_{H^+}$ is composed two components, ΔΨ and ΔpH, changes in luminal pH are negligible due to the small number of charge separations during the short pulse, and due to the strong pH buffering capacitance of the lumen [49]. The $\Delta\tilde{\mu}_{H^+}$ pre-existing in the dark, $\Delta\tilde{\mu}_{H^+dark}$, is in thermodynamic equilibrium with the [ATP]/([ADP]*[Pi]) ratio [48]. Accordingly, (A) $\Delta\tilde{\mu}_{H^+dark}$ is high when the ratio is high and (B) *vice versa*. The $\Delta\tilde{\mu}_{H^+dark}$ can be seen as a pedestal onto which the probed ΔΔΨ is superimposed [31]. The maximal ΔΔΨ, $\Delta\Delta\Psi_{max}$, is equivalent in its absolute value in between samples. Accordingly, the initial decay of ECS signals with variable amplitude can be compared. Black and red bars indicate darkness and actinic red light, respectively.

opposing particularities of the two F_1 systems were observed in basal ATPase activities and ADP inhibition properties: Compared to the corresponding wild type, the $F_{1\text{-redox}}$γMLCA was highly active and sulfite had an inhibiting effect. Additionally, the wild type ATPase activity showed an opposite response to H_2O_2 treatment: While hybrid F_1 ATPase activity is inhibited by H_2O_2 [17], $F_{1\text{-redox}}$ ATPase activity was enhanced (Fig. 1E). Nevertheless, in both systems the γMLCA mutants were responding less to the H_2O_2 treatment. Interestingly, $F_{1\text{-redox}}$γR279Q was as insensitive to H_2O_2 as the $F_{1\text{-redox}}$γMLCA.

Opposed to spinach CF_1 and the hybrid F_1 [17], ATPase activity stimulation by H_2O_2 in the $F_{1\text{-redox}}$ wild type as well as higher basal ATPase activity upon γMLCA could result from particularities of the cyanobacterial *T. elongatus* BP-1 enzyme. Taken together, the coinciding change of ADP inhibition properties in ROS-tolerant mutant F_1 enzyme suggests that the ROS impact on the wild type modulates ADP inhibition, as suggested in the model in Fig. 1F. The ionic track, involving rotation-guiding interactions between negatively charged βDELSEED motif residues and γArg/Lys [8], was modified in $F_{1\text{-redox}}$γR279Q. ROS-mediated oxidation of the γMet/Cys targets might influence βGlu/Asp interactions of the DELSEED motif with γArg279. Thus, a change in mechanistic properties could modulate ADP inhibition. For instance, when restricting relative movements of the γ-termini in *T. elongatus* BP-1 F_1 $\alpha_3\beta_3\gamma$ by engineered disulfides, ADP inhibition was low and high ATPase activity was observed [24]. A similar, ROS-mediated restriction could result in elevated ATPase activity upon H_2O_2 treatment in $F_{1\text{-redox}}$ (Fig. 1E) and a modification of γ-terminal movements could have caused inhibition of the spinach enzyme [17]. However, understanding of the ROS impact on F_1 is purely based on *in vitro* studies. Despite earlier studies on isolated thylakoids using photosensitizers [22], it is not known whether the ROS-mediated CF_1F_o modification occurs *in vivo* as well. The mutated γArg described in $F_{1\text{-redox}}$γR279Q is highly conserved. Since ATPase redox regulation was not disturbed in the mutant, site-directed mutagenesis was carried out in the photosynthetic model organism *Chlamydomonas reinhardtii* to analyze CF_1F_o modulation by ROS *in vivo*.

3.2. Laser flash-induced electrochromic shift measurements of *C. reinhardtii* cells revealed enhanced H_2O_2 resistance in CF_1F_o γR277Q

Based on the observations in Fig. 1, the transition to an *in vivo* model was made by generating *Chlamydomonas reinhardtii* CF_1F_o γR277Q, referred to as γR277Q. The mutation did not interfere with phototrophic growth and transformants were cultured on minimum medium. Due to modified pigment absorbance spectra in the presence of an electric field, photosynthetic membranes are spectroscopic voltmeters [reviewed in 6]. Generated by light-driven electron transfer and H^+ translocation processes, the electrochromic shift (ECS) of the pigments serves as a probe for the electric field component (ΔΨ) of the *trans*-thylakoid electrochemical proton gradient $\Delta\tilde{\mu}_{H^+}$. The flash-induced ECS decay kinetics is multi-phasic and has been used for decades to monitor ATP synthesis in a non-invasive manner [2,4,38]. It comprises three phases: a fast phase of increase corresponding to charge separations in photosystems ("a" phase), a second phase of increase corresponds to the electrogenic activity of the cytochrome b_6f complex which generates an additional electric field [6] ("b" phase), and a phase of ECS decay which is mainly due to ATP synthesis by H^+ translocation *via* CF_1F_o. ECS decay rates at the end of the "b" phase were used for ATP synthesis activity calculations, referred to as CF_1F_o activity hereafter for simplicity (Methods, Section 2.4). It is important to note that the rate of H^+ translocation *via* CF_1F_o also modifies the kinetics and amplitude of the "b" phase because the two phases partly overlap. The slower the CF_1F_o-mediated decay of the electric field, the more pronounced the electrogenic activity of the cytochrome b_6f complex appears [6]. This was previously clearly revealed in a CF_1F_o-lacking strain [4]. We noticed a faster flash-induced ECS decay in dark-adapted mutant samples (Fig. 2A), suggesting higher CF_1F_o activity in the mutant. Accordingly, amplitude and duration of the "b" phase in the 20 ms-range after the flash (gray indication in Fig. 2A) were more pronounced in the wild type. We ruled out that higher ECS decay rates in the mutant could be independent from CF_1F_o activity, *e.g.*, caused by a partial H^+ leak. The

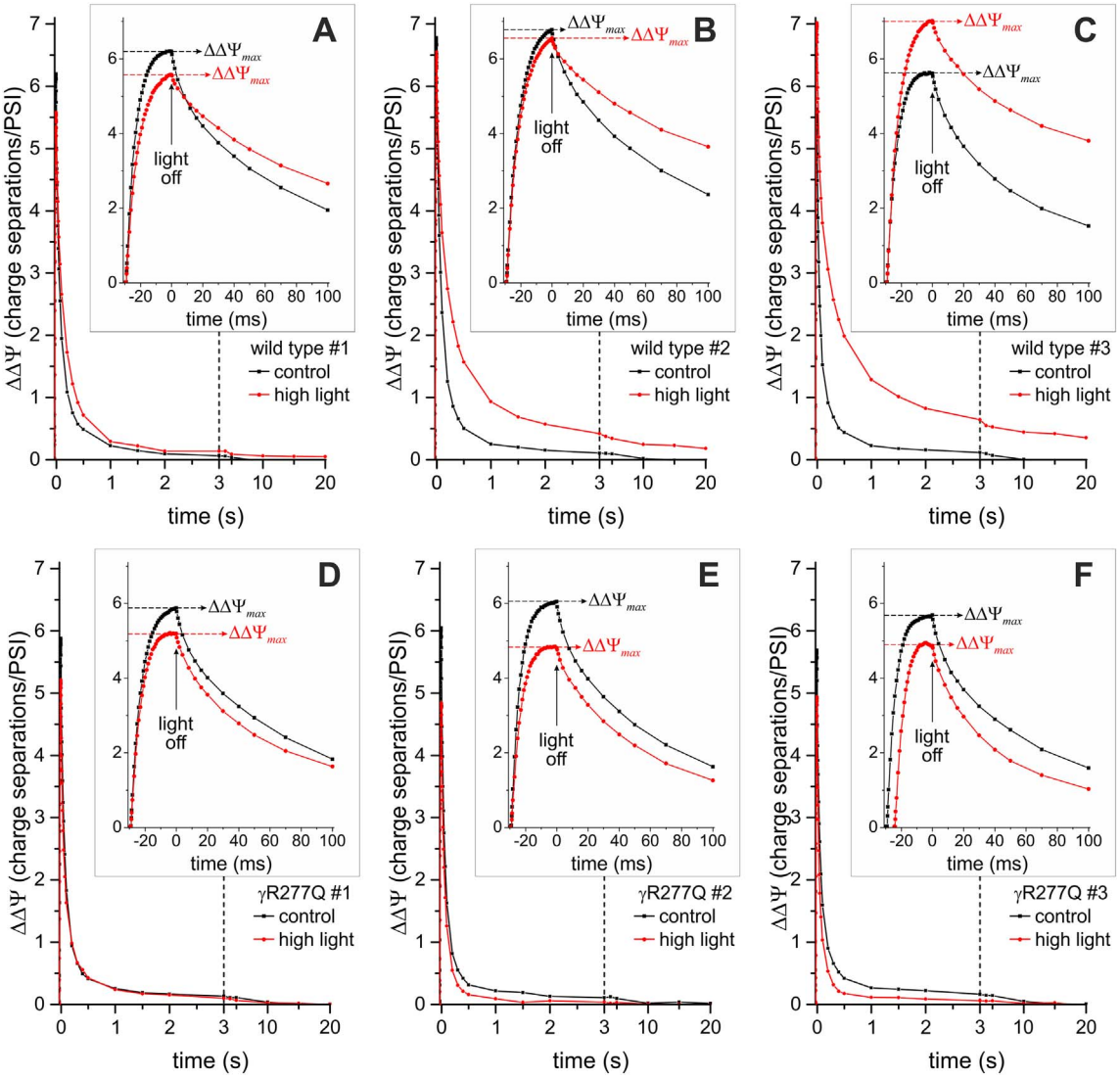

Fig. 6. The decay of the membrane potential generated by a short saturating light pulse in *C. reinhardtii* cells grown in low light and after high light treatment. Samples were dark-adapted and illumination by the saturating light pulse ended at time 0 when the maximal membrane potential, $\Delta\Delta\Psi_{max}$, was obtained (see insets). Following the pulse, a multi-phasic membrane potential decay was observed. Kinetics for independent wild type transformants (A–C) and γR277Q transformants (D–F) are shown. The ECS decay in high light-treated, $\Delta\tilde{\mu}_H{}^+$-activated wild type CF_1F_o was slowed down and produced long-living ECS signals. This was not observed in the mutant. For more details refer to the text in Section 3.4.

H^+ translocation *via* CF_o, which depends on de −/protonation of a Glu in the rotating c-subunits, is inhibited by CF_o-binding venturicidin [39]. ECS decay in the presence of venturicidin, reflecting the CF_1F_o-independent decay of the ΔΨ, was similar in wild type and mutant, and the amplitude and duration of the "b" phase were enhanced in the same manner (Fig. S2). This demonstrates that the faster ECS decay measured in the mutant was likely linked to higher CF_1F_o activity.

To test whether the *in vitro* findings in $F_{1\text{-redox}}$γR279Q can be applied to *C. reinhardtii* γR277Q, H_2O_2 was added to the cells. This treatment slowed down flash-induced ECS decay significantly, in both wild type (Fig. 2B) and the mutant (Fig. 2C). Photochemistry was not impaired because charge separations by a single-turnover laser flash were not altered during the experiment. This was demonstrated in dark-adapted samples by the constant values of light-induced ΔΨ changes (ΔΔΨ) during the unresolved "a" phase (~1.8 charge separations/PSI). Based on the approximate half-time of the ECS decay in the controls, the H_2O_2 impact after several minutes of treatment was about half as much in the mutant (Fig. 2D).

We concluded that, under the conditions tested, γR277Q rendered CF_1F_o twice as tolerant to H_2O_2 *in vivo*. Clearly, 5 mM H_2O_2 was beyond physiological relevance and monitoring for longer periods was aggravated by optically drifting samples. As a next step, we wanted to use a more physiological ROS-generating treatment by testing whether high light could lead to a similar effect, promoting oxidative modifications of CF_1F_o in a less artificial manner.

3.3. High light exposure slowed down wild type CF_1F_o activity

Before analysis, the cultures were transferred from growth condition light to high light (800 μmol photons $m^{-2}\,s^{-1}$) for 90 min, which promoted oxidative damage of the photosynthetic machinery. Chlamydomonas is routinely exposed to high light as a prerequisite for nonphotochemical fluorescence quenching measurements [40] and, as shown recently [41], expression of PSII repair cycle proteins is upregulated under high light stress, in conditions that were harsher than in our experiments. We chose a 90-min treatment and effects began to evolve at 30 min (Fig. S3). Based on parameter assessments of both photosystems, major damage occurred at PSII in all strains at similar extents. No significant differences were observed in loss of PSI and redox parameters of P700 during the applied photoinhibition period (Fig. 3, Table 1).

Photoinhibition resulted in a smaller number of charge separations

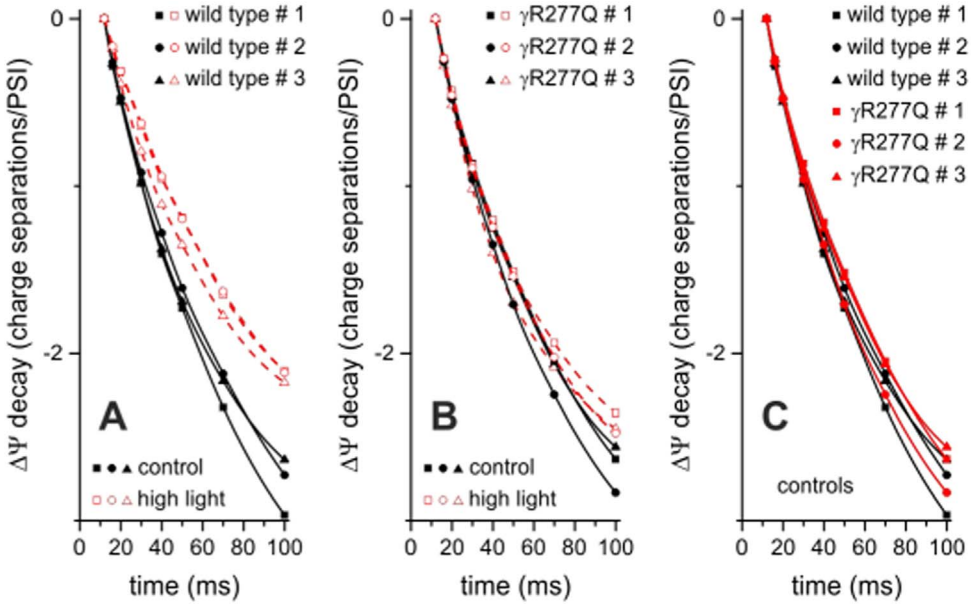

Fig. 7. Comparison of initial ΔΨ decay. As indicated in Fig. 5, ECS decay kinetics can be compared with each other. After $\Delta\Delta\Psi_{max}$ was obtained, the electrogenic activity of the cytochrome b_6f complex during the first ms of the decay gave rise to an underestimation of the CF_1F_o contribution. Therefore, ΔΔΨ values at 12 ms in the dark were set to 0 after cytochrome b_6f complex ceased to be active, disregarding earlier events. (A) Slowdown of the initial ΔΨ decay after high light treatment of *C. reinhardtii* wild type cells is shown with kinetics taken from Fig. 6. (B) The initial ΔΨ decay in the mutant was almost not compromised. (C) The controls showed similar ΔΨ decay kinetics. The short illumination transitioned CF_1F_o into a $\Delta\tilde{\mu}_{H^+}$-activated conformation. The samples produced larger initial ECS decay amplitudes in the activated state, compared to Fig. 4 after membrane energization by a laser flash.

upon a single-turnover laser flash (Table 1). When comparing the high light-induced loss of charge separations per PSI, both wild type and γR277Q were photoinhibited similarly (see also Fig. 4). However, the ECS kinetics after the high light treatment was clearly different between the two strains. In the wild type, the ECS decay phase was slower after high light and the "b" phase was significantly increased in amplitude (Fig. 4A). Such a change in the shape of the ECS cannot be explained by the decreased "a" phase. Indeed, the comparison of the ECS kinetics following a saturating flash or a non-saturating flash (yielding different "a" phase amplitudes) indicate that both treatments resulted in homothetic kinetics (Fig. S4). Instead, as described in the introduction, the two observations were both consequences of a slowdown of the CF_1F_o activity. Interestingly, the ECS decay in the high light-exposed wild type re-accelerated after certain minutes in darkness (Fig. S5). However, this observation will be explored in more detail elsewhere.

The pronounced slowdown of the ECS decay beyond the "b" phase as in high light-treated wild type was not observed in the mutant (Fig. 4B). Such an observation strongly suggests that the physiological effect of ROS is the CF_1F_o slowdown and that the γArg mutation appeared to increase ROS resistance *in vivo*, too. Slowing down H^+ release from the lumen *via* CF_1F_o could be important for generating a high $\Delta\tilde{\mu}_{H^+}$, thus mediating efficient responses to high light. These could include the photosynthetic control, *i.e.*, the slowdown of the cytochrome b_6f [42] or the high energy quenching of the chlorophyll fluorescence, qE [43], which are both regulated by the luminal pH. However, at this stage, conclusions on CF_1F_o activity drawn from flash-induced ECS decay kinetics should be drawn with care. Indeed, the rate of CF_1F_o activity depends on other parameters including the regulation by its substrate, the $\Delta\tilde{\mu}_{H^+}$ (see Introduction). Since the $\Delta\tilde{\mu}_{H^+}$ across laser flash-energized membranes in dark-adapted cells was low, the $\Delta\tilde{\mu}_{H^+}$ regulation of CF_1F_o, initially demonstrated by membrane energization with consecutive short laser flashes [2], was not contributing to our observations. ATPase activity measurements in isolated chloroplasts showed that $\Delta\tilde{\mu}_{H^+}$ stimulated the rate-limiting product release [44], *i.e.*, $\Delta\tilde{\mu}_{H^+}$ cancels ADP inhibition – the feature that was altered by the mutation *in vitro*. During the ATP synthesis mode, the main energy-consuming steps of ATP release and Pi binding [45] might be facilitated in laser flash-energized membranes harboring mutant CF_1F_o. The γR277Q mutation as well as the actual ROS targets are found in a CF_1F_o region that was structurally responding to $\Delta\tilde{\mu}_{H^+}$ [46]. In a physiological scenario under high light, ROS formation coincides with a high $\Delta\tilde{\mu}_{H^+}$. Therefore, CF_1F_o should be in its $\Delta\tilde{\mu}_{H^+}$-activated state when it is supposedly slowed down by ROS. To test whether the activated enzyme is also slowed down by ROS, we modified the protocol and measured CF_1F_o activity after generating a significant $\Delta\tilde{\mu}_{H^+}$ by short illumination.

3.4. After transitioning into the $\Delta\tilde{\mu}_{H^+}$-activated CF_1F_o conformation, the membrane potential decayed slower via the high light-treated wild type enzyme

A recently described method allowed us to monitor the generation of a membrane potential in dark-adapted samples by illuminating for several milliseconds with a saturating light pulse [31]. Before presenting the results, it is necessary to point out that in the dark, the $\Delta\tilde{\mu}_{H^+}$ is not null and a certain level, $\Delta\tilde{\mu}_{H^+dark}$, is maintained *via* ATP hydrolysis in the dark [47]. As proposed by Junge [48] and summarized in Fig. 5, the $\Delta\tilde{\mu}_{H^+dark}$ is in equilibrium with the [ATP]/([ADP]*[P_i]) ratio. If the [ATP]/([ADP]*[P_i]) ratio is low, the $\Delta\tilde{\mu}_{H^+dark}$ will be low. On the contrary, if the ratio is high, the $\Delta\tilde{\mu}_{H^+dark}$ will be high, too. A critical threshold $\Delta\tilde{\mu}_{H^+}$, $\Delta\tilde{\mu}_{H^+trigger}$, needs to be exceeded to promote high CF_1F_o activity rates [2,48]. Regarding the method that we used here, three considerations are given:

1. It is assumed that in dark-adapted samples the pulse-generated change of $\Delta\tilde{\mu}_{H^+}$ ($\Delta\Delta\tilde{\mu}_{H^+}$) mainly reflects a light-induced change of its electric component ΔΨ (ΔΔΨ), considering the relatively small number of charge separations during the ms-pulse in combination with the high buffering capacitance of the lumen [49]. The latter feature made changes in ΔpH negligible in first approximation.
2. A sufficiently large ΔΔΨ during the ms-pulse energized the membrane above the critical $\Delta\tilde{\mu}_{H^+trigger}$, promoting high CF_1F_o activity. The pulse duration was adjusted to reach a maximal ΔΔΨ (indicated as $\Delta\Delta\Psi_{max}$ in Fig. 6 insets).
3. Equal absolute ΔΨ values were obtained at the end of the pulse (measured as $\Delta\Delta\Psi_{max}$), exclusively depending on the electric permeability of the membrane [31].

Since inhibition of the photosynthetic apparatus after high light treatment was similar in the samples (Fig. 3, Table 1) one could assume that it is valid to calibrate each sample internally by PSI, as for the flash-induced kinetics shown before (see Methods, Section 2.4).

Following the pulse, ECS signals decayed slower in the high light-treated wild type transformant lines (Fig. 6A–C). In addition, a very slow phase of variable amplitude with a lifetime > 20 s was observed.

After high light, the ΔΔΨ dissipation in the mutant was less compromised and the slow phase was not observed (Fig. 6D–F). In the following discussion, we advise to refer to Fig. 5 as well: In wild type and mutant controls (Fig. 6), the ΔΔΨ had similar amplitudes, reaching comparable $\Delta\Delta\Psi_{max}$ values. This implied that in the dark-adapted samples, given the thermodynamic equilibrium with the [ATP]/([ADP]*[P_i]) ratio, the pre-existing $\Delta\tilde{\mu}_{H^+dark}$ was comparable. Accordingly, the mutation did not cause a partial H^+ leak *via* CF_1F_o which would otherwise lower both the [ATP]/([ADP]*[P_i]) ratio and $\Delta\tilde{\mu}_{H^+dark}$. When comparing high light samples with controls, none of the treated mutants produced larger ΔΔΨ amplitudes – unlike the wild type. This points to the direction that in wild type #3, for instance, slightly lower plastidic ATP levels contributed to a smaller $\Delta\tilde{\mu}_{H^+dark}$. However, the high light effects on the ΔΔΨ amplitudes were variable in the wild type lines and conclusions should be drawn carefully. Following high light treatment, chloroplast ATP levels in dark-adapted samples depend on various processes such as ATP-consuming PSII repair [50], in addition to mitochondrial respiration rates [51]. We are aware that the calibration method could become ambiguous if the high light-induced abundance of field-indicating pigments was altered. Instead of the internal reference, high light-treated samples were calibrated to signals produced by one charge separation per PSI in the corresponding control, given equal cell concentrations (Fig. S6). However, the basic conclusions were the same.

Considering that equal absolute ΔΨ values were obtained at the end of the pulse, CF_1F_o activities were compared. The initial CF_1F_o-related decay phase could not be measured unbiased due to an overlap with cytochrome b_6f activity after switching off the light, in analogy to the "b" phase described for flash-induced ECS decay above. Therefore, the first 12 ms of the decay were disregarded, the ΔΔΨ value at 12 ms darkness was set to 0, and the ΔΨ decay up to 100 ms is shown in Fig. 7. In line with findings preformed with laser flashes, the compromised wild type (Fig. 7A) and unvaried mutant (Fig. 7B) clearly demonstrate that CF_1F_o inhibition by high light treatment was independent of the $\Delta\tilde{\mu}_{H^+}$, revealing that ROS did impair both the performance of the $\Delta\tilde{\mu}_{H^+}$-activated and the non-activated CF_1F_o conformation. The relatively large ECS decay amplitudes during the initial phase confirmed that the $\Delta\tilde{\mu}_{H^+}$-activated CF_1F_o conformation was obtained in both enzymes (Fig. 7C).

4. Conclusions and outlook

ROS production is an inevitable process during photosynthesis. The capacity to detoxify the reactive intermediates depends on the physiological state of the cell and can be surpassed during the high light treatment like the one we used here, favoring oxidative damage of various cellular components. Our *in vivo* ATP synthase analysis, which started as an *in vitro* study and used independent Chlamydomonas transformants, presents evidence that the CF_1F_o function is compromised under high light stress that favors ROS production. Functional impairment most likely resulted from oxidation events in the γ-subunit neck region, harboring previously identified ROS target residues [17]. This could result in mechanistic modifications during rotational catalysis which were bypassed in the mutant. We propose that ROS could play a regulatory role by modifying CF_1F_o. Given that the substrate of CF_1F_o, the $\Delta\tilde{\mu}_{H^+}$, is also the main regulator of the high light responses in the photosynthetic electron transfer chain, the potential of a ROS-modified CF_1F_o in the feedback-regulated photosynthetic apparatus could be important, too. Indeed, both the high light response mechanisms at the PSII level and the photosynthetic control at the cytochrome b_6f level are regulated by the ΔpH, the osmotic component of the $\Delta\tilde{\mu}_{H^+}$. Two main questions remain to be answered and will be examined in future studies. First, the regulations at the level of PSII and cytochrome b_6f depend on the H^+ conductivity of CF_1F_o. For example, under CO_2-limiting and fluctuating light conditions, highly conductive Arabidopsis CF_1F_o with point mutations in the γ-subunit had an impact on the photosynthetic machinery [52,53]. These experimental conditions were, in part, described to be favorable for ROS production but modification of CF_1F_o by ROS was not considered. It will be interesting to test whether the mutation of our study produces similar results. Second, it is tempting to propose that the temporary inhibition in wild type CF_1F_o involves enzymatic repair mechanisms, such as the Met sulfoxide reductase system [reviewed in 54]. This repair mechanism would ensure transient control of PSII and cytochrome b_6f by a ROS-modulated CF_1F_o and will be examined elsewhere.

Transparency document

The http://dx.doi.org/10.1016/j.bbabio.2017.09.001 associated with this article can be found, in online version.

Acknowledgements

We would like to thank Francis-André Wollman and Pierre Joliot for stimulating discussions and help during the preparation of the manuscript. This work was supported in part by a Postdoctoral Fellowship for Foreign Researchers from the Japan Society for the Promotion of Science (P12389) (to F. B.) and the Core Research of Evolutional Science and Technology program from the Japan Science and Technology Agency (to T. H.). Parts of the work were funded by an ERC Starting Grant PhotoPHYTOMICS (ERC-2016-STG 715579) (to B. B).

Appendix A. Supplementary data

Supplementary data to this article can be found online at http://dx.doi.org/10.1016/j.bbabio.2017.09.001.

References

[1] W. Junge, N. Nelson, ATP synthase, Annu. Rev. Biochem. 84 (2015) 631–657.
[2] W. Junge, B. Rumberg, H. Schroder, The necessity of an electric potential difference and its use for photophosphorylation in short flash groups, Eur. J. Biochem. 14 (1970) 575–581.
[3] U. Junesch, P. Graber, Influence of the redox state and the activation of the chloroplast ATP synthase on proton-transport-coupled ATP synthesis hydrolysis, Biochim. Biophys. Acta 893 (1987) 275–288.
[4] P. Joliot, R. Delosme, Flash-induced 519 nm absorption change in green algae, Biochim. Biophys. Acta 357 (1974) 267–284.
[5] D.M. Kramer, A.R. Crofts, Activation of the chloroplast ATPase measured by the electrochromic change in leaves of intact plants, Biochim. Biophys. Acta 976 (1989) 28–41.
[6] B. Bailleul, P. Cardol, C. Breyton, G. Finazzi, Electrochromism: a useful probe to study algal photosynthesis, Photosynth. Res. 106 (2010) 179–189.
[7] J.P. Abrahams, A.G. Leslie, R. Lutter, J.E. Walker, Structure at 2.8 Å resolution of F_1-ATPase from bovine heart mitochondria, Nature 370 (1994) 621–628.
[8] J.P. Ma, T.C. Flynn, Q. Cui, A.G.W. Leslie, J.E. Walker, M. Karplus, A dynamic analysis of the rotation mechanism for conformational change in F_1-ATPase, Structure 10 (2002) 921–931.
[9] K.R. Dunham, B.R. Selman, Regulation of spinach chloroplast coupling factor 1 ATPase activity, J. Biol. Chem. 256 (1981) 212–218.
[10] Z.Y. Du, P.D. Boyer, On the mechanism of sulfite activation of chloroplast thylakoid ATPase and the relation of ADP tightly bound at a catalytic site to the binding change mechanism, Biochemistry 29 (1990) 402–407.
[11] S.D. Dunn, R.G. Tozer, V.D. Zadorozny, Activation of *Escherichia coli* F_1-ATPase by lauryldimethylamine oxide and ethylene glycol: relationship of ATPase activity to the interaction of the ε and β subunits, Biochemistry 29 (1990) 4335–4340.
[12] M.L. Richter, W.J. Patrie, R.E. McCarty, Preparation of the ε subunit and ε subunit-deficient chloroplast coupling factor-1 in reconstitutively active forms, J. Biol. Chem. 259 (1984) 7371–7373.
[13] J.D. Mills, P. Mitchell, P. Schurmann, Modulation of coupling factor ATPase activity in intact chloroplasts - the role of the thioredoxin system, FEBS Lett. 112 (1980) 173–177.
[14] Y. Kim, H. Konno, Y. Sugano, T. Hisabori, Redox regulation of rotation of the cyanobacterial F_1-ATPase containing thiol regulation switch, J. Biol. Chem. 286 (2011) 9071–9078.
[15] F. Buchert, H. Konno, T. Hisabori, Redox regulation of CF_1-ATPase involves interplay between the γ-subunit neck region and the turn region of the βDELSEED-loop, Biochim. Biophys. Acta 1847 (2015) 441–450.
[16] J.Z. Pu, M. Karplus, How subunit coupling produces the γ subunit rotary motion in F_1-ATPase, Proc. Natl. Acad. Sci. U. S. A. 105 (2008) 1192–1197.
[17] F. Buchert, Y. Schober, A. Rompp, M.L. Richter, C. Forreiter, Reactive oxygen

species affect ATP hydrolysis by targeting a highly conserved amino acid cluster in the thylakoid ATP synthase γ subunit, Biochim. Biophys. Acta 1817 (2012) 2038–2048.
[18] K. Apel, H. Hirt, Reactive oxygen species: metabolism, oxidative stress, and signal transduction, Annu. Rev. Plant Biol. 55 (2004) 373–399.
[19] A.H. Mehler, Studies on reactions of illuminated chloroplasts. 2. Stimulation and inhibition of the reaction with molecular oxygen, Arch. Biochem. Biophys. 34 (1951) 339–351.
[20] M. Takahashi, K. Asada, Superoxide production in aprotic interior of chloroplast thylakoids, Arch. Biochem. Biophys. 267 (1988) 714–722.
[21] M.J. Davies, The oxidative environment and protein damage, Biochim. Biophys. Acta 1703 (2005) 93–109.
[22] F. Buchert, C. Forreiter, Singlet oxygen inhibits ATPase and proton translocation activity of the thylakoid ATP synthase CF_1CF_O, FEBS Lett. 584 (2010) 147–152.
[23] N.N. Nichols, C.S. Harwood, PcaK, a high-affinity permease for the aromatic compounds 4-hydroxybenzoate and protocatechuate from *Pseudomonas putida*, J. Bacteriol. 179 (1997) 5056–5061.
[24] E. Sunamura, H. Konno, M. Imashimizu, M. Mochimaru, T. Hisabori, A conformational change of the γ subunit indirectly regulates the activity of cyanobacterial F_1-ATPase, J. Biol. Chem. 287 (2012) 38695–38704.
[25] J. Weber, S.T. Hammond, S. Wilke-Mounts, A.E. Senior, Mg^{2+} coordination in catalytic sites of F_1-ATPase, Biochemistry 37 (1998) 608–614.
[26] J.M. Jault, C. Dou, N.B. Grodsky, T. Matsui, M. Yoshida, W.S. Allison, The $\alpha_3\beta_3\gamma$ subcomplex of the F_1-ATPase from the thermophilic *Bacillus* PS3 with the βT165S substitution does not entrap inhibitory MgADP in a catalytic site during turnover, J. Biol. Chem. 271 (1996) 28818–28824.
[27] O. Landt, H.P. Grunert, U. Hahn, A general method for rapid site-directed mutagenesis using the polymerase chain reaction, Gene 96 (1990) 125–128.
[28] D. Drapier, B. Rimbault, O. Vallon, F.A. Wollman, Y. Choquet, Intertwined translational regulations set uneven stoichiometry of chloroplast ATP synthase subunits, EMBO J. 26 (2007) 3581–3591.
[29] D.S. Gorman, R.P. Levine, Cytochrome *f* and plastocyanin: their sequence in the photosynthetic electron transport chain of *Chlamydomonas reinhardtii*, Proc. Natl. Acad. Sci. U. S. A. 54 (1965) 1665–1669.
[30] C. Raynaud, C. Loiselay, K. Wostrikoff, R. Kuras, J. Girard-Bascou, F.A. Wollman, Y. Choquet, Evidence for regulatory function of nucleus-encoded factors on mRNA stabilization and translation in the chloroplast, Proc. Natl. Acad. Sci. U. S. A. 104 (2007) 9093–9098.
[31] P. Joliot, A. Joliot, Quantification of the electrochemical proton gradient and activation of ATP synthase in leaves, Biochim. Biophys. Acta 1777 (2008) 676–683.
[32] W. Junge, H.T. Witt, On the ion transport system of photosynthesis—investigations on a molecular level, Z. Naturforsh. B 23 (1968) 244–254.
[33] B. Genty, J.-M. Briantais, N.R. Baker, The relationship between the quantum yield of photosynthetic electron transport and quenching of chlorophyll fluorescence, Biochim. Biophys. Acta Gen. Subj. 990 (1989) 87–92.
[34] H. Takahashi, S. Clowez, F.A. Wollman, O. Vallon, F. Rappaport, Cyclic electron flow is redox-controlled but independent of state transition, Nat. Commun. 4 (2013) 1954.
[35] C. Klughammer, U. Schreiber, An improved method, using saturating light-pulses, for the determination of photosystem-I quantum yield via $P700^+$-absorbency changes at 830nm, Planta 192 (1994) 261–268.
[36] K. Shin, R.K. Nakamoto, M. Maeda, M. Futai, F_oF_1-ATPase γ subunit mutations perturb the coupling between catalysis and transport, J. Biol. Chem. 267 (1992) 20835–20839.
[37] M. Sobti, C. Smits, A.S. Wong, R. Ishmukhametov, D. Stock, S. Sandin, A.G. Stewart, Cryo-EM structures of the autoinhibited *E. coli* ATP synthase in three rotational states, Elife 5 (2016).
[38] B. Rumberg, U. Siggel, Quantitative relationship between chlorophyll-b reaction, electron transport and phosphorylation during photosynthesis, Z. Naturforsh. B 23 (1968) 239–244.
[39] S. Zhang, D.D. Letham, A.T. Jagendorf, Inhibition of thylakoid ATPase by venturicidin as an indicator of CF_1CF_o interaction, Plant Physiol. 101 (1993) 127–133.
[40] K.K. Niyogi, T.B. Truong, Evolution of flexible non-photochemical quenching mechanisms that regulate light harvesting in oxygenic photosynthesis, Curr. Opin. Plant Biol. 16 (2013) 307–314.
[41] F. Wang, Y. Qi, A. Malnoe, Y. Choquet, F.A. Wollman, C. de Vitry, The high light response and redox control of thylakoid FtsH protease in Chlamydomonas Reinhardtii, Mol. Plant 10 (2017) 99–114.
[42] C. Foyer, R. Furbank, J. Harbinson, P. Horton, The mechanisms contributing to photosynthetic control of electron transport by carbon assimilation in leaves, Photosynth. Res. 25 (1990) 83–100.
[43] G. Peers, T.B. Truong, E. Ostendorf, A. Busch, D. Elrad, A.R. Grossman, M. Hippler, K.K. Niyogi, An ancient light-harvesting protein is critical for the regulation of algal photosynthesis, Nature 462 (2009) 518–521.
[44] J.H. Kaplan, E. Uribe, A.T. Jagendorf, ATP hydrolysis caused by acid-base transition of spinach chloroplasts, Arch. Biochem. Biophys. 120 (1967) 365–370.
[45] P.D. Boyer, R.L. Cross, W. Momsen, A new concept for energy coupling in oxidative phosphorylation based on a molecular explanation of the oxygen exchange reactions, Proc. Natl. Acad. Sci. U. S. A. 70 (1973) 2837–2839.
[46] R.E. McCarty, J. Fagan, Light-stimulated incorporation of N-ethylmaleimide into coupling factor-1 in spinach chloroplasts, Biochemistry 12 (1973) 1503–1507.
[47] G. Finazzi, F. Rappaport, *In vivo* characterization of the electrochemical proton gradient generated in darkness in green algae and its kinetic effects on cytochrome b_6f turnover, Biochemistry 37 (1998) 9999–10005.
[48] W. Junge, The critical electric potential difference for photophosphorylation. Its relation to the chemiosmotic hypothesis and to the triggering requirements of the ATPase system, Eur. J. Biochem. 14 (1970) 582–592.
[49] W. Junge, W. Auslander, A.J. McGeer, T. Runge, The buffering capacity of the internal phase of thylakoids and the magnitude of the pH changes inside under flashing light, Biochim. Biophys. Acta 546 (1979) 121–141.
[50] A.K. Mattoo, H. Hoffman-Falk, J.B. Marder, M. Edelman, Regulation of protein metabolism: coupling of photosynthetic electron transport to in vivo degradation of the rapidly metabolized 32-kilodalton protein of the chloroplast membranes, Proc. Natl. Acad. Sci. U. S. A. 81 (1984) 1380–1384.
[51] P. Bennoun, Chlororespiration revisited: mitochondrial-plastid interactions in Chlamydomonas, Biochim. Biophys. Acta Bioenerg. 1186 (1994) 59–66.
[52] D. Takagi, K. Amako, M. Hashiguchi, H. Fukaki, K. Ishizaki, T. Goh, Y. Fukao, R. Sano, T. Kurata, T. Demura, S. Sawa, C. Miyake, Chloroplastic ATP synthase builds up a proton motive force preventing production of reactive oxygen species in photosystem I, Plant J. (2017).
[53] A. Kanazawa, E. Ostendorf, K. Kohzuma, D. Hoh, D.D. Strand, M. Sato-Cruz, L. Savage, J.A. Cruz, N. Fisher, J.E. Froehlich, D.M. Kramer, Chloroplast ATP synthase modulation of the thylakoid proton motive force: implications for photosystem I and photosystem II Photoprotection, Front. Plant Sci. 8 (2017) 719.
[54] A. Drazic, J. Winter, The physiological role of reversible methionine oxidation, Biochim. Biophys. Acta 1844 (2014) 1367–1382.